PROCEEDINGS OF SCIENCE

Measurements of CP violation in $B \to DD$ decays

Marta Calvi[*†]
Università di Milano Bicocca and INFN - Milano, Italy
E-mail: marta.calvi@mib.infn.it

Measurements of CP violation in beauty to double-charm decays performed at LHCb are presented. The violation of CP symmetry is observed for the first time in $B^0 \to D^{*+}D^-$ decays, while no evidence for CP violation is found in $B^- \to D^-_{(s)}D^0$ decays.

18th International Conference on B-Physics at Frontier Machines - Beauty2019 -
29 September / 4 October, 2019
Ljubljana, Slovenia

[*]Speaker.
[†]on behalf of the LHCb Collaboration

PoS(Beauty2019)008

The LHCb experiment has performed several studies of B meson decays to a pair of charmed mesons, using data collected during LHC Run 1 and Run 2. Examples are measurements of branching ratios in various charged and neutral double charm decay modes [1] and the determination of the mixing phases in $B^0 \to D^+D^-$ [2] and $B_s^0 \to D_s^+D_s^-$ decays [3]. [1] Tests of the Standard Model (SM) have been performed by relating CP asymmetries and branching fractions of different decay modes of neutral and charged decays of B mesons to two charmed mesons, employing isospin or SU(3) flavor symmetries [4]. New results of measurements of CP violating observables in $B^0 \to D^{*\pm}D^{\mp}$ decays [5] and recent measurements in $B^- \to D^-_{(s)}D^0$ decays [6] are presented.

The $B^0 \to D^{*\pm}D^{\mp}$ decay process is sensitive to the weak phase 2β, when the leading-order color-favoured tree diagram $b \to c\bar{c}d$ is considered, where $\beta \equiv \arg[-(V_{cd}V_{cb}^*)/(V_{td}V_{tb}^*)]$ is one of the angles of the Unitarity Triangle. The decay can proceed through other processes, like penguin, W-exchange and annihilation diagrams, where additional contributions to CP violation both from the SM and from new physics may arise. Each of the $D^{*+}D^-$ and $D^{*-}D^+$ final states is accessible from both B^0 and $\bar{B}^0$ mesons, therefore four decay rates are considered. The time-dependent decay rate for an initial B^0 meson to a $D^{*+}D^-$ final state is

$$\frac{\mathrm{d}\Gamma_{B^0,f}(t)}{\mathrm{d}t} = \frac{\mathrm{e}^{-t/\tau_d}}{8\tau_d}(1+\mathscr{A}_{f\bar{f}})\Big[1 - S_f \sin(\Delta m_d t) + C_f \cos(\Delta m_d t)\Big],$$

where the parameter $\mathscr{A}_{f\bar{f}}$, which represents the overall asymmetry in the production of the $f = D^{*+}D^-$ and $\bar{f} = D^{*-}D^+$ final states, is defined as

$$\mathscr{A}_{f\bar{f}} = \frac{\left(|A_f|^2 + |\bar{A}_f|^2\right) - \left(|A_{\bar{f}}|^2 + |\bar{A}_{\bar{f}}|^2\right)}{\left(|A_f|^2 + |\bar{A}_f|^2\right) + \left(|A_{\bar{f}}|^2 + |\bar{A}_{\bar{f}}|^2\right)},$$

with A_f ($A_{\bar{f}}$) and $\bar{A}_f$ ($\bar{A}_{\bar{f}}$) indicating the amplitudes of the decay of a B^0 and a $\bar{B}^0$ meson to the final state f ($\bar{f}$). Similar expressions describe the decay of a $\bar{B}^0$ meson and decays to the $\bar{f}$ final state. Here τ_d denotes the B^0 lifetime and Δm_d denotes the mass difference of the two B^0 mass eigenstates, which are assumed to have the same decay width [7]. Introducing q and p to describe the relation between mass and flavor eigenstates, $|B_{\mathrm{H,L}}\rangle = p|B^0\rangle \pm q|\bar{B}^0\rangle$, the parameters S_f and C_f are defined as

$$S_f = \frac{2\mathscr{I}m\lambda_f}{1+|\lambda_f|^2}, \qquad C_f = \frac{1-|\lambda_f|^2}{1+|\lambda_f|^2}, \qquad \lambda_f = \frac{q}{p}\frac{\bar{A}_f}{A_f},$$

with analogous definitions holding for $S_{\bar{f}}$, and $C_{\bar{f}}$. By combining these parameters, the following five CP observables for $B^0 \to D^{*\pm}D^{\mp}$ decays can be defined [7]

$$S_{D^*D} = \frac{1}{2}(S_f + S_{\bar{f}}),\ \Delta S_{D^*D} = \frac{1}{2}(S_f - S_{\bar{f}}),\ C_{D^*D} = \frac{1}{2}(C_f + C_{\bar{f}}),\ \Delta C_{D^*D} = \frac{1}{2}(C_f - C_{\bar{f}}),\ \mathscr{A}_{D^*D} = \mathscr{A}_{f\bar{f}}.$$

The measurements of these parameters are based on the full sample of pp collision data recorded by the LHCb experiment between 2011 and 2018, corresponding to integrated luminosities of 1 and 2 fb^{-1} at centre-of-mass energies of 7 and 8 TeV (Run 1) and of 6 fb^{-1} at 13 TeV (Run 2).

[1] Charge-conjugate processes are implicitly included in the following, unless otherwise specified.

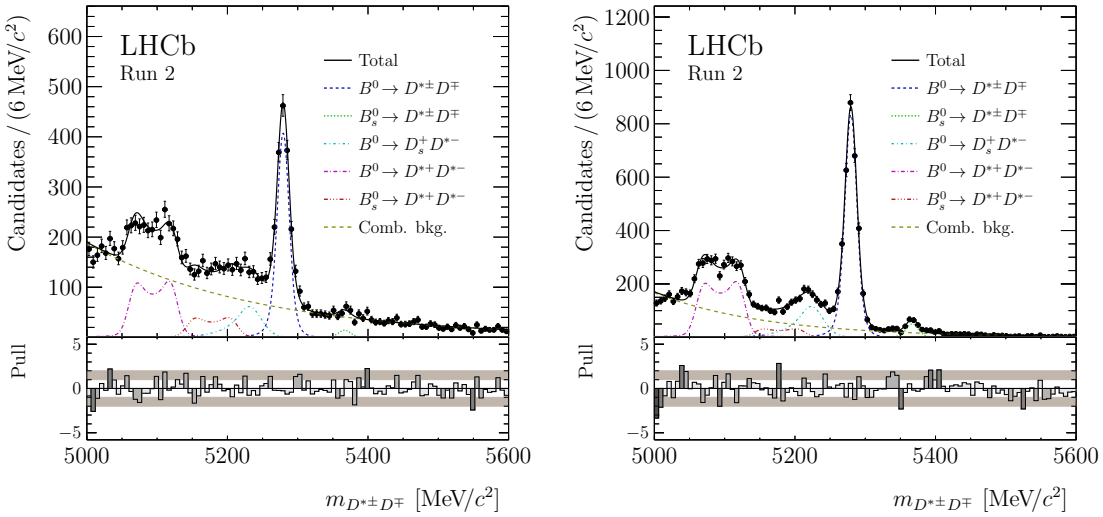

Figure 1: Invariant-mass distributions for the $B^0 \to D^{*+}D^-$ decay with (left) $D^0 \to K^-\pi^+\pi^-\pi^+$ and (right) $D^0 \to K^-\pi^+$, obtained using the Run 2 data samples. Besides the data points and the full PDFs (solid black) the projections of the B^0 signal (dashed blue), the $B_s^0 \to D^{*+}D^-$ background (dotted green), the $B^0 \to D^{*+}D_s^-$ background (dash-dotted turquoise), the $B^0 \to D^{*+}D^{*-}$ background (long-dash-dotted magenta), the $B_s^0 \to D^{*+}D^{*-}$ background (dash-three-dotted red) and the combinatorial background (long-dashed green) are shown.

The $B^0 \to D^{*+}D^-$ candidates are selected with the decay chain $D^- \to K^+\pi^-\pi^-$ and $D^{*+} \to D^0\pi^+$, with $D^0 \to K^-\pi^+$ and $D^0 \to K^-\pi^+\pi^-\pi^+$ decays. Kinematic, mass and particle-identification (PID) requirements are imposed to reject background due to the misidentification of one hadron in the charged D decay chain, such as $B^0 \to D^{*+}D_s^-(K^+K^-\pi^-)$ and $\overline{\Lambda}_b^0 \to D^{*+}\Lambda_c^-(K^+\bar{p}\pi^-)$ decays. Single-charm B meson decays, such as $B_{(s)}^0 \to D^{*+}h^-h^+h^-$, where the three hadrons are not produced in a D^- decay, but directly originate from the B decay, are also rejected. In order to separate further the signal candidates from the combinatorial background, a boosted decision tree (BDT) [8] that takes as inputs kinematical, topological and PID variables of all decay products is used. The BDT is trained using simulated $B^0 \to D^{*+}D^-$ candidates as a signal proxy, and data candidates in the high-mass sideband as a background proxy. A different BDT classifier is trained for each of the four data samples (two D^0 decay modes, two run periods), and the requirement on the output is chosen to minimise the uncertainties on the CP violating parameters.

An unbinned extended maximum-likelihood fit is performed on the invariant-mass distribution of the selected B^0 candidates, for each of the four data samples independently. The *sPlot* technique [9] is employed to determine per-candidate weights that are used for background subtraction in the subsequent decay-time fit. A total of about 6000 signal candidates are found in the four data samples. The mass distributions for the Run 2 samples are shown in Fig. 1.

The measurement of CP violation in a decay-time-dependent analysis of a neutral beauty meson decay requires the determination of the production flavor of the B^0 meson candidate, i.e. whether it contained a b or a $\overline{b}$ quark (flavor-tagging). Two classes of tagging algorithms are used in this analysis. The opposite-side (OS) tagger exploits the fact that b and $\overline{b}$ quarks are almost exclusively produced in pairs in pp collisions, allowing the flavor of the signal B^0 candidate to be

inferred from the flavor of the other b hadron in the event. The OS tagger combines information on the charge of the muon or electron from semileptonic b decays, the charge of the kaon from the $b \to c \to s$ decay chain, the charge of a reconstructed secondary charm hadron and the charges of the tracks that form the secondary vertex of the other b-hadron decay [10, 11]. The same-side (SS) tagger exploits the production of correlated protons or pions in the hadronization of the $\overline{b}$ (b) quark that forms the signal B^0 ($\bar{B}^0$) candidate, with its initial flavor identified by the charge of the particle [12]. Each tagging algorithm provides a tagging decision and the probability that it is incorrect (mistag, ω). Large data samples of flavor-specific decays, such as $B^+ \to J/\psi K^+$ and $B^0 \to D^-\pi^+$ are used to optimize the algorithms and calibrate the mistag probabilities of each tagger. In this analysis, the combination of OS and SS algorithms is calibrated using data samples of $B^0 \to D^{*+}D_s^-$ and $B^0 \to D^+D_s^-$ decays. These decays are chosen because they are flavor-specific decays with similar topology and kinematics as the signal decay and with high yields. The performance of the flavor tagging is given by the tagging power, $\varepsilon_{\rm tag}D^2$, where $\varepsilon_{\rm tag}$ is the fraction of tagged candidates and $D = 1-2\omega$ represents the dilution induced on the oscillation amplitude. The tagging power represents the effective loss in signal yield compared to a perfectly tagged sample. The tagging power for the combination of the OS and SS algorithms in the signal sample is found to be $5.6-7.1\%$, depending on the data sample. This is among the highest tagging powers measured at LHCb, benefiting from the high p and and p_T values of the selected B^0 candidates.

An unbinned maximum-likelihood fit is performed to the decay-time distribution of background-subtracted candidates, simultaneously to the four data samples of tagged and untagged candidates. The decay-rate PDF includes terms dependent on the flavor tagging parameters (efficiencies and mistag for the B^0 and $\bar{B}^0$ mesons) and on the $B^0-\bar{B}^0$ production asymmetry, that are Gaussian-constrained to the measurement performed in the $B^0 \to D^{(*)+}D_s^-$ control channels. The decay-time resolution model is determined from simulation and fixed in the fit to data with an effective resolution of 60 fs. The decay-time efficiency is modelled by a cubic spline function with five knots and coefficients determined in the fit to data. The B^0 lifetime and Δm_d are fixed to their known values [13]. Figure 2 shows the decay-time distribution of the full $B^0 \to D^{*\mp}D^{\pm}$ sample while Fig. 3 shows the asymmetry between $\bar{B}^0$ and B^0 signal yields as a function of the decay time, separately for $D^{*+}D^-$ and $D^{*-}D^+$ final states. The CP violating observables resulting from the decay-time fit are

$$\begin{aligned}
S_{D^*D} &= -0.861 \pm 0.077\,(\text{stat}) \pm 0.019\,(\text{syst}),\\
\Delta S_{D^*D} &= 0.019 \pm 0.075\,(\text{stat}) \pm 0.012\,(\text{syst}),\\
C_{D^*D} &= -0.059 \pm 0.092\,(\text{stat}) \pm 0.020\,(\text{syst}),\\
\Delta C_{D^*D} &= -0.031 \pm 0.092\,(\text{stat}) \pm 0.016\,(\text{syst}).
\end{aligned}$$

The statistical uncertainties include contributions due to the size of the samples and due to the external parameters constrained in the fit. The main statistical correlations are between S_{D^*D} and C_{D^*D} ($\rho_{S,C} = 0.44$) and between ΔS_{D^*D} and ΔC_{D^*D} ($\rho_{\Delta S,\Delta C} = 0.46$). Systematic uncertainties on the CP violating parameters are evaluated by considering the variation of the mass model, both for the signal and background components, and the variation of the flavor tagging calibration model. The uncertainties related to the knowledge of the decay-time acceptance and decay-time resolution,

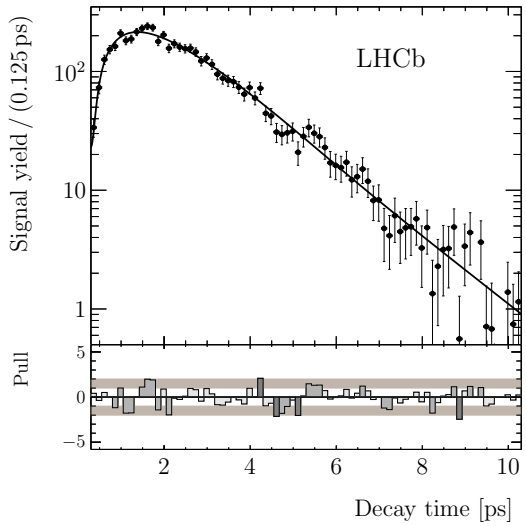

Figure 2: Decay-time distribution of $B^0 \to D^{*\mp}D^{\pm}$ signal candidates, summed over all data samples, where the background contribution is subtracted by means of the *sPlot* technique. The projection of the PDF is represented by the solid line.

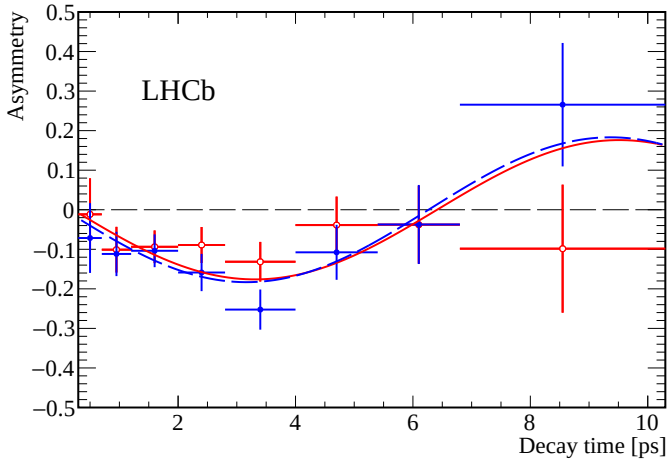

Figure 3: Asymmetry between $\bar{B}^0$ and B^0 signal yields as a function of the decay time, for (blue full dot) $D^{*+}D^-$ and (red empty dot) $D^{*-}D^+$ tagged signal candidates. The background contribution is subtracted by means of the *sPlot* technique. The corresponding projections of the PDF are represented by the blue dashed (red continuous) line. The B^0 flavor is determined by the combination of all flavor-tagging algorithms.

and those related to the uncertainties on the input parameters in the decay-time model give small contributions.

The final state raw asymmetry, which is also determined from the decay-time fit, has to be corrected for instrumental asymmetries. These asymmetries affect reconstruction, detection and particle identification and are related to the different interaction cross-sections with matter and different detection and identification efficiencies of positive and negative pions and kaons. The re-

constructed $B^0 \to D^{*+}D^-$ decay is charge symmetric. However, since all instrumental efficiencies depend on momenta, and the p and $p_{\rm T}$ spectra of kaons and pions in the $D^{*\pm}$ and $D^{\mp}$ decays are observed to be slightly different, the cancellation is not expected to be complete. To a good level of approximation, the asymmetry in $B^0 \to D^{*+}D^-$ decays, denoted with $A_{\rm det}^{D^{*-}D^+}$, can be related to the D^{*-} and D^- instrumental asymmetries, $A_{\rm det}^{D^{*-}}$ and $A_{\rm det}^{D^-}$, as

$$A_{\rm det}^{D^{*-}D^+} \simeq A_{\rm det}^{D^{*-}} - A_{\rm det}^{D^-}\,.$$

Each of the D^{*-} and D^- asymmetries is measured using samples of prompt $D^- \to K^+\pi^-\pi^-$ decays, after a kinematic weighting of the distribution of the D^- final state particles to match the spectra of signal kaons and pions. The resulting asymmetries are very small: in Run 2 they are found to be $A_{\rm det}^{D^{*-}D^+} = 0.0011 \pm 0.0040 \pm 0.0030$ ($0.0009 \pm 0.0026 \pm 0.0051$) in the $D^0 \to K^-\pi^+$ ($D^0 \to K^-\pi^+\pi^+\pi^+$) decay mode, where the first uncertainty is statistical and the second is systematic. After subtracting the instrumental asymmetries, the weighted mean of the final state asymmetries is evaluated over the four samples resulting in

$$\mathscr{A}_{D^*D} = 0.008 \pm 0.014\ (\text{stat}) \pm 0.006\ (\text{syst}).$$

The main contributions to the systematic uncertainty on $\mathscr{A}_{D^*D}$ comes from the uncertainty on the instrumental asymmetries and from the variation of the mass model.

These results on the $B^0 \to D^{*\pm}D^{\mp}$ CP violating parameters are compatible with previous measurements performed by the Belle [14] and BaBar [15] experiments and exclude the hypothesis of CP conservation at more than 10 standard deviations. The precision of C_{D^*D} and ΔC_{D^*D} parameters is comparable with that of previous measurements, while for S_{D^*D}, ΔS_{D^*D} and $\mathscr{A}_{D^*D}$, this measurement improves significantly the precision of the current world average [7].

The measurements of the CP asymmetries in $B^- \to D^-D^0$ and $B^- \to D_s^-D^0$ decays are performed at LHCb with Run 1 data [6]. In these decay modes of charged B mesons, non-zero CP asymmetries are expected due to the interference of the tree and loop amplitudes, at O(10^{-2}) in the SM. The time-integrated CP asymmetry is defined as

$$\mathscr{A}^{\rm CP} = \frac{\Gamma(B^- \to D_{(s)}^-D^0) - \Gamma(B^+ \to D_{(s)}^+\bar{D^0})}{\Gamma(B^- \to D_{(s)}^-D^0) + \Gamma(B^+ \to D_{(s)}^+\bar{D^0})}$$

and it is measured from the yield of selected signal candidates. Charmed mesons are reconstructed in the $D^- \to K^+\pi^-\pi^-$ and $D_s^- \to K^+K^-\pi^-$ decay modes, while D^0 mesons are reconstructed in the $D^0 \to K^-\pi^+$ and $D^0 \to K^-\pi^+\pi^-\pi^+$ decay modes. The mass distribution of the B^- and B^+ candidates are shown in Fig. 4, for the two-body D^0 decay samples. The raw asymmetries need to be corrected for production and detection asymmetries. The production asymmetry between B^- and B^+ mesons at LHCb has been measured using the $B^- \to D^0\pi^-$ decay to be $A_{\rm P} = (-0.5 \pm 0.4)\%$ [16], with no significant dependence of the asymmetry on the transverse momentum or on the rapidity of the B meson. Four contributions to the asymmetry of the detection efficiencies are considered: asymmetries in the tracking efficiency, different kaon interaction cross-sections with the detector material, and asymmetries in the trigger and particle identification efficiencies. These asymmetries are evaluated using control samples of fully and partially reconstructed D^{*+}

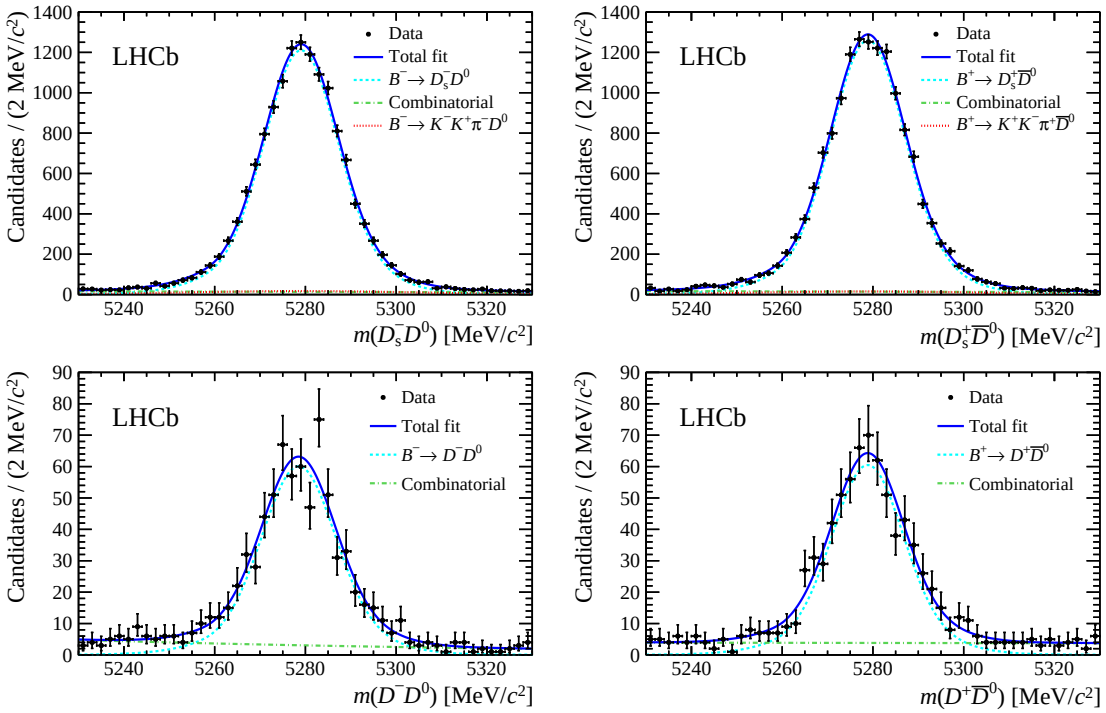

Figure 4: Invariant-mass distribution of (top) $B^- \to D_s^- D^0$ and (bottom) $B^- \to D^- D^0$ candidates, with $D^0 \to K^- \pi^+$, separated by charge. The left plots are for B^- candidates whereas the right plots are for B^+ candidates. The overlaid curves show the signal (dashed turquoise) and the combinatorial background (dash-dotted green) components of the PDF. In the $B^- \to D_s^- D^0$ decay also a single charm background (dotted red) component is present.

decays [17] and of $D^+ \to K^- \pi^+ \pi^+$ and of $D^+ \to K_S \pi^+$decays [18]. The uncertainties on the contributions to the production and detection asymmetries are considered to be uncorrelated, and values of $A_P + A_{det}$ equal to $(-1.4 \pm 0.5)\%$ and $(-0.3 \pm 0.4)\%$ are obtained for $B^- \to D_s^- D^0$ and $B^- \to D^- D^0$ decays, respectively. The CP asymmetries are measured to be

$$\begin{aligned} \mathscr{A}^{CP}(B^- \to D_s^- D^0) &= (-0.4 \pm 0.5\,(\text{stat}) \pm 0.5\,(\text{syst}))\%\,, \\ \mathscr{A}^{CP}(B^- \to D^- D^0) &= (2.3 \pm 2.7\,(\text{stat}) \pm 0.4\,(\text{syst}))\%\,. \end{aligned}$$

This is the first measurement of $\mathscr{A}^{CP}(B^- \to D_s^- D^0)$ and the most precise determination of $\mathscr{A}^{CP}(B^- \to D^- D^0)$. Neither result shows evidence for CP violation.

In conclusion, beauty to double-charm decays have been successfully studied at LHCb. The violation of CP symmetry has been observed in $B^0 \to D^{*+} D^-$ decays, while no evidence for CP violation has been found in $B^- \to D_{(s)}^- D^0$ decays. The full exploitation of the Run 2 data sample for double-charm decays has not been performed yet. The importance of these channels will increase in the upcoming Run 3, with the LHCb upgraded detector, due to the removal of that hardware trigger, which limited the trigger efficiency in hadronic channels. The future LHCb-Upgrade Phase 2, proposed for the High-Luminosity LHC era, will allow all statistical uncertainties in the measurements of these decays to be further reduced.

References

[1] LHCb collaboration, R. Aaij *et al. Measurement of the $B_s^0 \to D_s^{(*)+} D_s^{(*)-}$ branching fractions*, Phys. Rev. D93, 092008 (arXiv:1602.07543). LHCb collaboration, R. Aaij *et al. First observations of $B_s^0 \to D^+D^-, D_s^+D^-$ and $D^0\bar{D}^0$ decays* Phys. Rev. D87 (2013) 092007 (arXiv:1302.5854).

[2] LHCb collaboration, R. Aaij *et al. Measurement of CP violation in $B^0 \to D^+D^-$ decays*, Phys. Rev. Lett. 117 (2016) 261801 (arXiv:1608.06620).

[3] LHCb collaboration, R. Aaij *et al. Measurement of the CP-violating phase ϕ_s in $B_s^0 \to D_s^+D_s^-$ decays*, Phys. Rev. Lett. 113 (2014) 211801(arXiv:1409.4619).

[4] M. Jung and S. Schacht, *Standard Model Predictions and New Physics Sensitivity in $B \to DD$ decays* Phys. Rev. D91,034027 (arXiv:1410.8396); L. Bel, K. DeBruyn, R. Fleisher *et al. Anatomy of $B \to D\bar{D}$ decays* JHEP 1507 (2015) 108 (arXiv:1204.1735).

[5] LHCb collaboration, R. Aaij *et al. Measurement of the CP violation in $B^- \to D^{*\pm}D^{\mp}$ decays* LHCb-PAPER-2019-036, submitted to JHEP, arXiv:1912.03723.

[6] LHCb collaboration, R. Aaij *et al. Measurement of the CP asymmetry in $B^- \to D_s^-D^0$ and $B^- \to D^-D^0$ decays* JHEP 05 (2018) 160 (arXiv:1803.10990).

[7] Heavy Flavor Averaging Group, Y. Amhis *et al.*, *Averages of b-hadron, c-hadron, and τ-lepton properties as of summer 2016*, Eur. Phys. J. **C77** (2017) 895 (arXiv:1612.07233) updated results and plots available at https://hflav.web.cern.ch.

[8] Y. Freund and R. E. Schapire, *A decision-theoretic generalization of on-line learning and an application to boosting*, J. Comput. Syst. Sci. **55** (1997) 119

[9] M. Pivk and F. R. Le Diberder, *sPlot: A statistical tool to unfold data distributions*, Nucl. Instrum. Meth. **A555** (2005) 356 (arXiv:0402083).

[10] LHCb collaboration, R. Aaij *et al. Opposite-side flavour tagging of B mesons at the LHCb experiment* Eur. Phys. J. **C72** (2012) 2022 (arXiv:1202.4979).

[11] LHCb collaboration, R. Aaij *et al. B flavour tagging using charm decays at the LHCb experiment* JINST 10 (2015) P10005 (arXiv:1507.07892).

[12] LHCb collaboration, R. Aaij *et al. New algorithms for identifying the flavour of B^0 mesons using pions and protons* Eur. Phys. J. **C77** (2017) 238 (arXiv:1610.06019).

[13] Particle Data Group, M. Tanabashi *et al.*, *Review of particle physics*, Phys. Rev. **D98** (2018) 030001.

[14] Belle collaboration, M. Rohrken *et al.*, *Measurements of branching fractions and time-dependent CP violating asymmetries in $B^0 \to D^{(*)\pm}D^{\mp}$decays*, Phys. Rev. D.85.091106 (arXiv:1203.6647).

[15] BaBar collaboration, B. Aubert *et al.*, *Measurements of time-dependent CP asymmetries in $B^0 \to D^{(*)+}D^{(*)-}$ decays*, Phys. Rev. D.79.032002 (arXiv:0808.1866).

[16] LHCb collaboration, *et al. Measurement of the $B^{\pm}$ production asymmetry and the CP asymmetry in $B^{\pm} \to J\psi K^{\pm}$ decays*, Phys. Rev. D 95 (2017) 052005 (arXiv:1701.05501).

[17] LHCb collaboration, R. Aaij *et al. Measurement of the $D_s^+D_s^-$ production asymmetry in 7 TeV pp collisions* Phys. Lett. B713 (2012) 186 (arXiv:1205.0897).

[18] LHCb collaboration, R. Aaij *et al. Measurement of CP asymmetry in $D^0 \to K^-K^+$ and $D^0 \to \pi^-\pi^+$ decays* JHEP 07 (2014) 041 (arXiv:1405.2797).